A R C H I V E S O F M E T A L L U R G Y A N D M A T E R I A L S
Volume 51 2006 Issue 4

G. MRÓWKA-NOWOTNIK* J. SIENIAWSKI*, A. NOWOTNIK*

INTERMETALLIC PHASE IDENTIFICATION ON THE CAST AND HEAT TREATED 6082 ALUMINIUM ALLOY

CHARAKTERYSTYKA FAZ MIĘDZYMETALICZNYCH W STOPIE ALUMINIUM 6082 W STANIE LANYM I PO OBRÓBCE CIEPLNEJ

In the technical 6xxx Al alloys besides the intentional additions Mg and Si transition metals and impurities (Fe and Mn) are always present. Even not large amount of these impurities causes the formation a new phase components: Al-Fe, Al-Fe-Si and Al-Fe-Mn-Si. During casting of 6xxx alloys, a wide variety of Fe-containing complex intermetallic phases, i.e.: β-Al_5FeSi, α-$Al_{15}(FeMn)_3Si$), Al_9Mn_3Si and Mg_2Si, are formed among the dendrite arms of α-Al solid solution. These intermetallics have different unit cell structures, morphologies, stabilities and physical properties depending on chemical composition and cooling conditions. Thus, these affects very much the mechanical properties of an alloy. In this study, several methods were used such as: optical light microscopy (LOM), transmission (TEM) and scanning (SEM) electron microscopy in combination with electron dispersive X-ray (EDX) using polished sample, and X-ray diffraction (XRD) to identify chemical composition and morphologies of the phase components in both as-cast and heat treated 6082 alloy.

Keywords: aluminium alloys, intermetallic phase, microscope observations, X-ray diffraction

W technicznych stopach aluminium grupy 6xxx obok podstawowych pierwiastków stopowych Mg i Si występują zawsze metale przejściowe oraz zanieczyszczenia przede wszystkim Fe i Mn. Mała ich zawartość powoduje już powstanie odrębnych faz międzymetalicznych Al-Fe, Al-Fe-Si oraz Al-Fe-Mn-Si. Ustalono, że podczas krzepnięcia stopów 6xxx tworzą się, w przestrzeniach międzydendrytycznych roztworu stałego α-Al, wydzielenia złożonych faz międzymetalicznych: β-Al_5FeSi, α-$Al_{15}(FeMn)_3Si$), Al_9Mn_3Si i Mg_2Si. W zależności od składu chemicznego oraz warunków chłodzenia zmienia się ich struktura, morfologia a także właściwości fizyczne, a to z kolei silnie wpływa na właściwości mechaniczne stopów. W pracy podjęto próbę identyfikacji faz międzymetalicznych występujących w stopie aluminium 6082. Zastosowano różne techniki badawcze (mikroskopia świetlna, transmisyjna mikroskopia elektronowa (TEM), elektronowa mikroskopia skaningowa z dyspersją energii promieniowania rentgenowskiego (SEM/EDX) oraz rentgenografia XRD), które umożliwiły określenie zmiany składu chemicznego i morfologii składników fazowych stopu w stanie lanym oraz po obróbce cieplnej.

1. Introduction

The 6xxx series aluminium alloys have widespread application, especially in the marine, automotive and air industry due to their excellent properties. The main alloying elements – Si and Mg, are partly dissolved in the primary α-Al matrix, and partly present in the form of intermetallic phases. A range of different intermetallic phases may form during solidification, depending on an alloy composition and solidification conditions. Relative volume fraction, chemical composition and morphology of the structural constituents exert significant influence on their useful properties [1–5]. Fe is present as an impurity in all commercial alloys [6]. During casting of 6xxx aluminium alloys a wide variety of Fe-containing intermetallics such as Al-Fe (Al_6Fe – orthorombic) and Al-Fe-Si (α-Al_8Fe_2Si – hexagonal, "Chinese script" and β-Al_5FeSi – monoclinic, platelike) may occur. Manganese increases the alloy strength either in solid solution or as a finely precipitated intermetallic. Manganese combines with Fe, Si and Al form an Al-Fe-Mn-Si intermetallic phase (α-$Al_{15}(FeMn)_3Si$ – cubic, "Chinese script"). A cast billets require a homogenization treatment to make the material suitable for hot extrusion. During this homogenization treatment several processes take place such as the transformation of interconnected plate-like β-Al_5FeSi intermetallics into more rounded discrete α_c-$Al_{15}(FeMn)_3Si$ particles and the dissolution of β-Mg_2Si particles [7, 8].

The addition of Mg to Al-Si alloys makes them heat treatable and allows for substantial increase in strength

* RZESZÓW UNIVERSITY OF TECHNOLOGY, 35-959 RZESZÓW, 2 WINCENTEGO POLA STR., POLAND

without reducing the corrosion resistance. The maximum solubility of Mg_2Si is 1.85% (at ~585°C) and decreases with decreasing temperature. Precipitation upon age hardening occurs via the formation of GP zones and metastable precursors of the equilibrium $\beta(Mg_2Si)$ [7, 9–10].

2. Material and experimental

The investigation has been carried out on the commercial 6082 aluminum alloy. The chemical composition of the alloy is: 1.2%Si, 0.78%Mg, 0.5%Mn, 0.33%Fe, 0.14%Cr, 0.08%Cu, 0.05%Zn, Al bal. The alloy was melted in an electrical resistance furnace and cast in an iron mould. The specimens were remelted at 750°C in ceramic crucible in air furnace. After being kept for 10 min at the temperature for melting the material entirely homogenizing the composition. The melted alloys were than cooled in the furnance at the cooling rate of 2°C/min.

The microstructure of examined alloy was observed using an optical microscope – Nikon 300 on polished sections etched in Keller solution (0.5% HF in 50ml H_2O). Thin foils for TEM studies were manufactured by cutting 3 mm diameter discs, followed by grinding manually to a thickness of about 0.1 mm. Finally, the disc was thinned electrolytically using a Struers Tenupol jet polishing machine, with a solution (by volume) CH_3OH (84cm^3), $HClO_4$ (3.5 cm^3) and glycerin (12.5 cm^3), operating at −10°C and U = 28V. The thin foils were examined in a Tesla BS-540 and JEOL – JEM 2010 ARP TEM/STEM operated at 200kV electron microscope. Morphology of specimens was made in the scanning electron microscope STEREOSCAN 420 (SEM), operating at 6–10 kV in a conventional back-scattered electron mode. Chemical composition of the intermetallics was made by EDS attached to the TEM using the software of an Oxford Link Isis 300 system. Qualitative analysis of the microstructure components of 6082 alloy was performed by X-ray diffraction (XRD), Thermo ARL diffractometer). The temperature of homogenization treatment was determined on the basis of literature data and calorimetric investigations. The samples were preheated in an induction furnace to a temperature 570°C, held for 6 hours and slow cooled in furnace. The T6 thermal processing of 6082 alloy was started by a heat treatment at the temperature of uniform α solid solution. Thus the all specimens were heated in a resistance furnace for 4 hours at 575°C and water-quenched. Subsequently the specimens were subjected to artificial aging at temperature of 175°C for 25 h.

3. Results and discussion

Fig. 1 shows as-cast microstructure of the investigated alloy. It consists of α-Al plus several morfologically distinct intermetallic constituents as well as Si phase. The typical as-cast microstructure of 6082 consists of a mixture of β-AlFeSi and α-AlFeMnSi intermetallic distributed at the α-Al interdendritic regions connected with coarse Mg_2Si, and a solid solution within the cells. The utilization of different etching methods allow to identify these intermetallic phases as: β-Al_5FeSi (dark phase), α-$Al_{15}(FeMn)_3Si$ (grey phase), Al_9Mn_3Si (light grey phase), Mg_2Si (black phase) (Fig. 1).

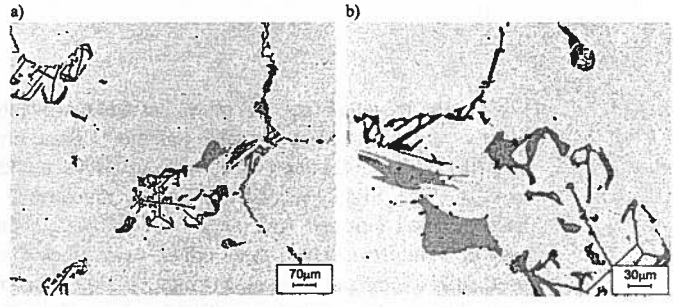

Fig. 1. As-cast microstructure of 6082 alloy

Since it is rather difficult to produce detailed identification of intermetallic using only one method (e.g. microscopic examination) therefore XRD technique was utilized to provide confidence in the results of phase classification based on metallographic study. The results of this investigation are showed in Fig. 2. X-ray diffraction analysis of 6082 alloy confirmed metalograffic observation. Results of the examination showed that the microstructure is mainly composed of: β-Al_5FeSi, α-$Al_{15}(FeMn)_3Si$, Al_9Mn_3Si and Mg_2Si phases.

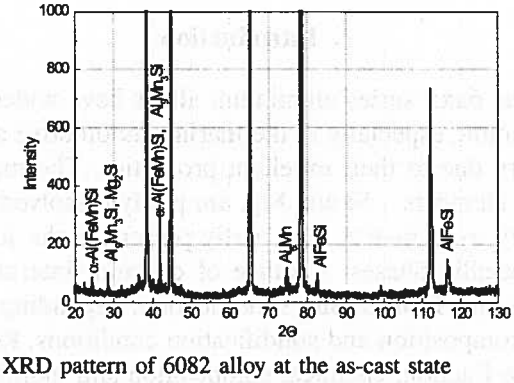

Fig. 2. XRD pattern of 6082 alloy at the as-cast state

Optical examination of the as-cast microstructure revealed the presence of Mg_2Si phase particles (Fig. 3, 4). The Mg_2Si phase can be readily identified according to its colour and morphology. Darker Mg_2Si particles, in the as-cast state after slow cooling rate – 2°C/min, precipitate in the form of lamellar or "Chinese script" struc-

ture (Fig. 3). These intermetallic phases are the products of binary eutectic reactions L → α-Al + Mg_2Si which occur at temperature 577°C [11]. When the eutectic composition is reached at the interface front, the ternary eutectic reaction L → α-Al + β-AlFeSi + Mg_2Si take place (Fig. 4).

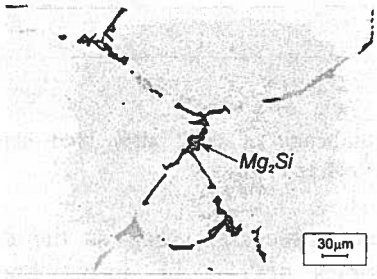

Fig. 3. The eutectic microstructure of α-Al + Mg_2Si

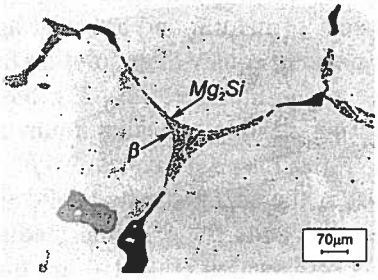

Fig. 4. Microstructure of 6082 alloy formed through the ternary eutectic reaction L → α-Al + β-AlFeSi + Mg_2Si

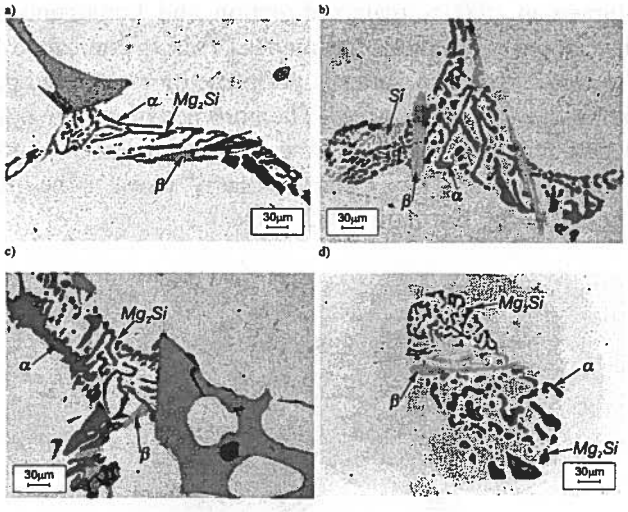

Fig. 5. As-cast microstructure of 6082 alloy: a-c) ternary eutectic d) the round ternary eutectic

The alloy in as-cast state consists some complex eutectic structures as well (Fig. 5). Moreover, the spherical in shape eutectic particles were also observed (Fig. 5d). It was found that three phases, namely: β-Al_5FeSi, Mg_2Si and α-$Al_{15}(FeMn)_3Si$ were present in the α-Al matrix (Fig. 5). These intermetallics grew together into a eutectic cluster.

During slow cooling rate 2°C/min after casting the β-Al_5FeSi with monoclinic crystal structure precipitates in the interdendritic regions generally as a plate-like morfology (Fig. 6).

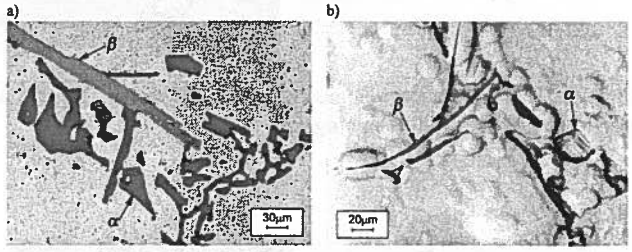

Fig. 6. Morphology of plate-like β-Al_5FeSi intermetallic phase (a) LM, (b) SEM micrograph

It is difficult to distinguish the intermetallic phases e.g. the β-Al_5FeSi, using classical metallographic technique. Therefore, besides light optical microscopy examination, SEM observation connected with EDS analysis of deep etched section were also made. The results of EDS analysis made on the coarse intermetallic phases are present in Table 1. Comparison of selected reference data to the results obtained by EDS scans showed good agreement between them (Table 1).

TABLE

Composition of the observed intermetallic phases (%wt)

Phase	Si	Fe	Mn	References
β-Al_5FeSi	12–15	25–30		[11]
	12,2	25		[12]
	14,59	27,75		[8]
	16,5	23,5		This work
α-$Al_{15}(FeMn)_3Si$	10–12	10–15	10–20	[11]
	5,5–6,5	5,1–27,9	14–24,7	[13]
	5–7	10–13	19–23	[14]
	10,8	5,2	18,29	This work

The β-Al_5FeSi phase with a plate-like morphology weaken the ductility and workability of 6xxx alloys. Due to the detrimental effect of the β-Al_5FeSi phase, their formation is avoided through additions of alloying elements, mainly of Mn and Be [15]. They alter the composition and morphology of β-plates into "Chinesse script", found mostly inside α-Al dendrites.

In the investigated 6082 alloy another common intermetallic α-$Al_{15}(FeMn)_3Si$ phase is present. The α-$Al_{15}(FeMn)_3Si$ phase, also known as α-Al_8Fe_2Si phase have a cubic structure and a compact morphology e.g. polyhedron (Fig. 7), which does not initiate cracks in the cast material to the same extent as the β-Al_5FeSi despite its elevated hardness.

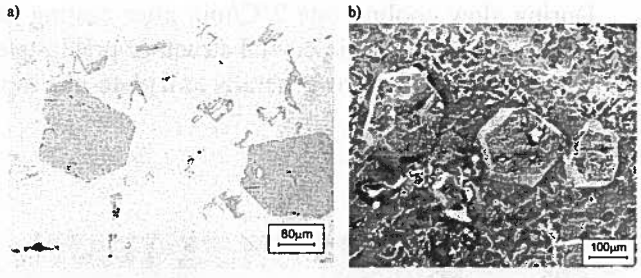

Fig. 7. Polyhedron morphologies of α-$Al_{15}(FeMn)_3Si$ intermetalic phase (a) LOM, (b) SEM micrograph

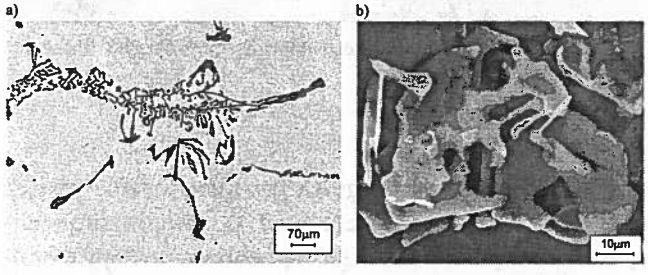

Fig. 8. "Chinese script" morphologies of α-$Al_{15}(FeMn)_3Si$ intermetalic phase (a) LOM, (b) SEM micrograph

When Mn and Mg are added to 6xxx alloys, e.g. 6082 alloy, the α-$Al_{15}(FeMn)_3Si$ is formed during solidification at the main eutectic and perytectic reaction [7, 16, 17]:

$$L \rightarrow \alpha\text{-Al} + \alpha\text{-}Al_{15}(FeMn)_3Si$$
$$L \rightarrow \alpha\text{-Al} + \alpha\text{-}Al_{15}(FeMn)_3Si + Mg_2Si$$
$$L + Al_6Mn(Fe) \rightarrow \alpha\text{-AlMnFeSi} + \alpha\text{-Al}$$
$$L + Al_3Fe \rightarrow \alpha\text{-AlMnFeSi} + \alpha\text{-Al}$$

The α-$Al_{15}(FeMn)_3Si$ phase shows, in contrast to the β-Al_5FeSi, some variations in composition and quite different morfologies depending on the cooling conditions. At low cooling rates the α-$Al_{15}(FeMn)_3Si$ phase is formed as a primary crystals. When cooling rate increases, those crystals changing morphology to a typical "Chinese script" form (Fig. 1, Fig. 8) or to a fine eutectic structure (Fig. 5).

In this work changes in the alloy microstructure after heat treatment were also observed. Fig. 9 shows the microstructure of 6082 alloy after homogenization heat treatment. During homogenization of the alloy at temperature 570°C for 6 hours, the transformation plate-like β-AlFeSi phase to more spheroidal α-$Al_{15}(FeMn)_3Si$ phase may occur. The transformation of β-AlFeSi phase to α-$Al_{15}(FeMn)_3Si$ intermetallic phase has been found to be important in these alloys. Kuijpers [18, 19] consider that an extradubility of 6xxx aluminium alloys increases due to the β to α transformation. The plate-like β-AlFeSi particles can lead to local crack initiation and induce surface defects on the extruded material. The more rounded α-$Al_{15}(FeMn)_3Si$ particles in the homogenized material improve the extradubility and surface quality of the extruded material.

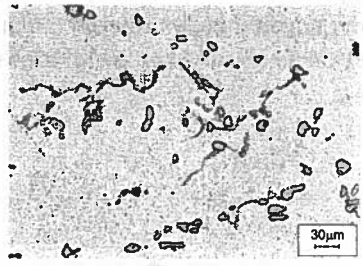

Fig. 9. Microstructure of 6082 alloy after homogenization at 570°C/6h and cooling in furnace

Additional processes, such as the dissolution of Mg_2Si particles also occur during homogenization. Quick cooling (in water or oil) after homogenization make possibility to solution heat treatment of the alloy. The process of natural and artificial ageing in 6082 alloy begin instantaneously after solution heat treatment. With respect to the literature [20–22], the precipitation sequence during heating the aluminium alloy 6082 is as follows: α (sss) $\rightarrow$ GP zones $\rightarrow$ β" $\rightarrow$ β' $\rightarrow$ β; where α (sss) is the supersaturated solid solution, GP – Guinier-Prestone zones, β", β' – intermediate metastable phases. TEM observation (Fig. 10) are quite similar to those observed previously by Broili [20] and Miao [22] and confirm above mentioned precipitation sequence. Fig. 10 shows fine needle-shaped β" phase particles aligned in <001> matrix direction and homogenously distributed throughout the matrix. This is confirmed by electron diffraction patterns performed for observed particles and the matrix areas. The presence of a large number of tiny dots represents the β" phase needles viewed end-on (Fig. 10). This indicates that β" phase is the main strengthening phase in 6082 alloy.

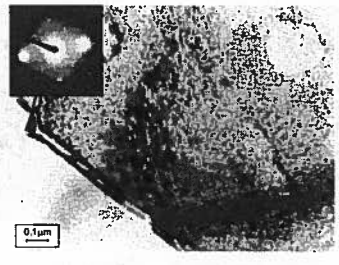

Fig. 10. TEM micrograph of 6082 alloy aged at 175°C for 6 h showing uniform dispersion of fine needle shaped β" particles

The microstructure of 6082 alloy after artificial ageing also contains spherical in shape fine particles (Fig. 11). These particles were analyzed using scanning transmission electron microscopy STEM and all of them were found to contain Al, Fe, Mn and Si suggesting that they were precipitates of α-$Al_{15}(FeMn)_3Si$ phase (Fig. 11).

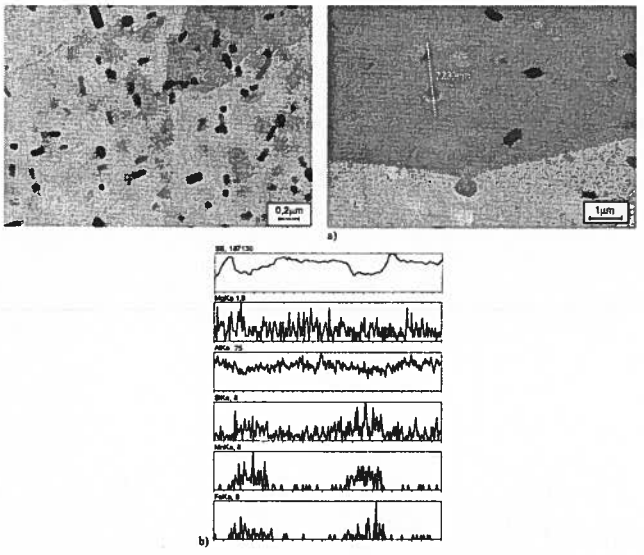

Fig. 11. STEM microstructure of 6082 alloy after precipitation hardening process showing dispersoid particles of AlFeMnSi phase (a,b) linear analysis of the chemical composition of spherical precipitates (c)

4. Conclusions

The alloy used in this study possessed a complex as-cast microstructure. By using various instruments (LOM, SEM, TEM/STEM, XRD) and techniques (imagine, EDS) a wide range of intermetallics phases were identified. After slow solidification at a cooling rate 2°C/min, the as-cast microstructure included six phases, namely: α-Al, β-Al_5FeSi, α-$Al_{15}(FeMn)_3Si$, Al_9Mn_3Si, Mg_2Si and Si. Depending on the composition and cooling rate of the alloy, the complex binary, ternary and quaternary eutectic structure in the solidified zone were also observed. During homogenization of 6082 alloy at temperature 570°C for 6 hours, the transformation of plate-like β-AlFeSi phase to more spheroidal α-$Al_{15}(FeMn)_3Si$ phase has been occurred. The microstructure of 6082 alloy after solution heat treatment and artificial ageing – T6, contain fine needle-shaped β" phase particles aligned in {001} matrix direction and homogenously distributed throughout the matrix. Additionally in the T6 condition spherical in shape fine particles of α-$Al_{15}(FeMn)_3Si$ phase were observed.

Acknowledgements

This work was carried out with the financial support of the Ministry of Science and Higher Education under grant No. 3T08A 048 30.

Received: 10 September 2006.

REFERENCES

[1] S. Karabay, M. Yilmaz, M. Zeren, J. Mater. Proc. Techn. **160**, 138–147 (2004).
[2] G. Mrówka-Nowotnik, J. Sieniawski, Proc. Int. Conf. "Achievements in Mechanical & Materials Engineering", 447–450, Gliwice-Wisła (2005).
[3] M. Warmuzek, J. Sieniawski, A. Gazda, G. Mrówka, Inż. Mat. **137**, 821–824 (2003).
[4] G. Mrówka-Nowotnik, J. Sieniawski, J. Mater. Proc. Techn. **367-372**, 162–163 (2005).
[5] S. Zajac, B. Bengtsson, Ch. Jönsson, Mater Sci Forum **396-402**, 675–680 (2002).
[6] M. Warmuzek, G. Mrówka, J. Sieniawski, J. Mater Proc Tech. **157-158**, 624–632 (2004).
[7] F. H. Samuel, A. M. Samuel, H. W. Doty, S. Valtierra, Metal and Mater Trans A. **32A** 2001–2061 (2000).
[8] Y. L. Liu, S. B. Kang, H. W. Kim, Mater Let. **41**, 267–272 (1999).
[9] A. K. Gupta, D. J. Lloyd, S. A. Court, Mater. Sci. Eng. **A301**, 140–146 (2001).
[10] G. A. Edwards, K. Stiller, G. L. Dunlop, M. J. Couper, Acta Mater. **46**, 11 3893–3904 (1998).
[11] L. F. Mondolfo, Aluminium Alloys: Structure and Properties. Butterworths, London-Boston, 1976.
[12] C. J. Simensen, P. Fartum, A. Andersen, Fres. Z. An. Chemistry **319**, 262–292 (1984).
[13] M. Warmuzek, K. Rabczak, J. Sieniawski, J. Mater. Proc. Techn. **162-163**, 422–428 (2005).
[14] V. Stefaniay, A. Griger, T. Turmezey, J. Mater. Sci. **22**, 539–546 (1987).
[15] S. R. Claves, D. L. Elias, W. Z. Misiolek, Mater. Sci. Forum **396-402**, 667–674 (2002).
[16] M. Warmuzek, A. Gazda, J. Sieniawski, G. Mrówka, Adv. Mater. Sci. 2, **4**, 81–91 (2003).
[17] M. Warmuzek. et al, Proc. Int. Conf. "Achievements in Mechanical & Materials Engineering" Gliwice-Zakopane 601–604 (2002).
[18] N. C. W. Kuijpers, W. H. Kool, P. T. G. Koenis, K. E. Nilsen, I. Todd, S. Van der Zwaag, Mater. Charact. **49**, 409–420 (2003).
[19] S. Spigarelli, E. Evangelista, H. J. McQueen, Scripta Mater. **49**, 179–183 (2003).
[20] G. Biroli, G. Caglioti, L. Martini, G. Riontino, Scripta Mater. **39**, 2, 197–203 (1998).
[21] L. Zhen, S. B. Kang, Mater. Let. **37**, 349–353 (1998).
[22] W. F. Miao, D. E. Laughlin, Scripta Mater. **40**, 7, 873–878 (1999).